STM JOURNALS

Journal of
Polymer & Composites

ISSN: 2321-2810 (Online)
ISSN: 2321-8525 (Print)
Volume 13, Special Issue 2, 2025
DOI (Journal): 10.37591/JoPC

https://journals.stmjournals.com/jopc

Research JoPC

Dielectric Studies Of 0.5Ba0.8Ca0.2TiO3.0.5CaCu3Ti4O12 Nanoceramic Fabricated by Chemo-Mechanical Process

Gajendra Singh Lodhi [1]*, Jyoti Sharma [2], Jayanta Kumar Mahato [3], Laxman Singh [4] and Atendra Kumar [5]

Abstract

The present investigation is aimed toward investigate a straightforward, inexpensive, and environmentally friendly chemo-mechanical method for preparing high-dielectric materials, specifically $0.5Ba_{0.8}Ca_{0.2}TiO_3.0.5CaCu_3Ti_4O_{12}$ (BCT-CCTO), by combining metal nitrate combustion with solid TiO_2 powder and titanium isopropoxide, Ti (OR)$_4$. The composite was prepared by the mixing of individual materials of $Ba_{0.8}Ca_{0.2}TiO_3$ and $CaCu_3Ti_4O_{12}$ through the chemo-mechanical method. Initially, 99% pure Ba $(NO_3)_3$, Cu $(NO_3)_2{\cdot}3H_2O$, TiO_2 and glycine were taken in their stoichiometry ratios. The composites were further sintered at 950ºC and 1000°C for 15 hrs. The presence of a major peak in BCT-CCTO composite at 1000°C 15 hrs. was investigated in the X-ray diffraction analysis which clearly confirmed the phase formation of BCT-CCTO composite. The surface morphology, the elemental homogenous composition of the element as a specific portion, and the electronic state of the metal ions of the BCT-CCTO composite were confirmed through SEM, EDX mapping, and XPS spectra respectively. It is observed that bimodal type of grain morphologies of several hundreds of nanometers are formed in the composites. It is also confirmed from TEM observation that the presence of spherical and homogenous-sized particles which resemble platelets of BCT-CCTO composite materials. Moreover, the results obtained at certain frequencies and temperatures are detailed in dielectric relaxation processes and because of interfacial polarization, a high dielectric constant was seen at low frequencies and high temperatures.

Keywords: X-ray diffraction, SEM, EDX, TEM, XPS, dielectric constant

***Author for Correspondence**
Gajendra Singh Lodhi

[1]Research Scholar, School of Basic and Applied Sciences, Shobhit Institute of Engineering and Technology (Deemed-to-be-University), Meerut, Uttar Pradesh., India
[2]Professor, School of Basic and Applied Sciences, Shobhit Institute of Engineering and Technology (Deemed-to-be-University), Meerut, Uttar Pradesh, India
[3]Associate Professor, School of Engineering and Technology, Shobhit Institute of Engineering and Technology (Deemed-to-be-University), Meerut, Uttar Pradesh, India
[4]Associate Professor, Department of chemistry, Siddharth University, Kapilvastu, Siddharth Nagar, Uttar Pradesh, India
[5]Professor, Department of Chemistry, Simdega College, Simdega (A constituent unit of Ranchi University), Jharkhand, India

Received Date: September 21, 2024
Accepted Date: December 23, 2024
Published Date: January 11, 2025

Citation: Gajendra Singh Lodhi, Jyoti Sharma, Jayanta Kumar Mahato, Laxman Singh Atendra Kumar. Dielectric Studies of 0.5Ba0.8Ca0.2TiO3.0.5CaCu3Ti4O12 Nanoceramic Fabricated by Chemo-mechanical Process. Journal of Polymer & Composites. 2025; 13(Special Issue 2): S12–S21p.

INTRODUCTION

The processing of nanomaterials has advanced recently, which has largely aided technological advancement. There are several uses for nano-composite materials, which are multi-component combinations of nano-dimensional phases with pronounced structural and chemical variations [1-9]. With respect to each constituent's structural, mechanical, electrical, electrochemical, and dielectric characteristics, these materials are composed of two or more inorganic phases. Because of their excellent processability, high breakdown field strength of metal oxides, and high dielectric constant of ABO_3 type oxides, nano-composite dielectrics are a very promising material for technological applications such as capacitors, microelectronics, and energy storage devices. All these desirable electrical and dielectric qualities are not found in a single substance. On the other hand, ABO_3 type oxide composites hold great potential as

high-performance dielectric material candidates since they can combine the oxide component's high dielectric constant with good thermal stability, high dielectric strength, and minimal increase in dielectric loss to improve the resulting energy density. $CaCu_3Ti_4O_{12}$ (CCTO) possesses a distorted cubic perovskite (ABO_3) structure with space group Im3 and a lattice parameter of 7.391 Å. The dielectric behavior of calcium copper titanate (CCTO) was first discovered by Subramanian et al. in 2000. A broad temperature range (100–600 K) is exhibited by this material, which also has an exceptionally high dielectric constant ($\varepsilon' \sim 10^4$–10^5) [10, 11]. They are extensively used in the manufacturing of automotive, aircraft, DRAM (Dynamic Random Access Memory), microwave devices, and multilayer capacitors, among other electronic components owing to possession of its high dielectric constant and also its low value of dielectric loss (tan δ) [12- 16]. Numerous studies on the dielectric characteristics of CCTO ceramic powder, single crystals, and related isomorphs have been published. However, the high loss tangent (tan δ) of CCTO ceramics (tan δ ~40.05 at 1 kHz) continues to be a major obstacle to the exploitation of applications requiring capacitive components (the large dielectric loss of CCTO normally beyond 3% is fatal). As a result, a great deal of study was conducted on how metal oxide additions such $ZnNb_2O_6$, $Pb(Zr_{0.52}Ti_{0.48})$, $BaTiO_3$, $CaTiO_3$, and $MgTiO_3$ might improve the dielectric characteristics of CCTO [17–21]. However, these authors did not find any appreciable improvements in the dielectric loss of the synthesized composites, even with the dielectric permittivity enhancement noted in each case.

These manuscripts have studied nano-composite materials of $0.5Ba_{0.8}Ca_{0.2}TiO_3.0.5CaCu_3Ti_4O_{12,}$ concerning different processing andpreparation conditions such as sol-gel derivation modified by the chemo-mechanical process at different sintering temperature and time. The sol-gel synthesis method is being explored and developed for the production of nanopowder materials including combustion, precipitation, mechanical, and chemo-mechanical methods. The sol-gelsynthesis method [22] of powder involves liquefying the reactants as a true solution. The found solution heated at high temperature changes to powder, after that powder materials are modified with the help of pastel mortar and converted to pellet form. This synthesis is a chemo-mechanical method. The shapes and sizes of grains of the materials depend on the parameters at which the process is conducted and usually, pellets with a few grains of nanometer size are obtained by this route. This method is useful for coating films. $Ba_{0.8}Ca_{0.2}TiO_3$ ceramic has shown a large dielectric constant and low tan delta value. Research must investigate that, the composition of the composite materials exhibits large dielectric constant and low tan delta value at higher frequency.

A details comparison of dielectric and other properties of $Ba_{0.8}Ca_{0.2}TiO_3CaCu_3Ti_4O_{12}$ (BCT-CCTO) nanoceramics with other ceramic materials are summarized in the following Table 1.

Experimental Procedure

The composite $0.5Ba_{0.8}Ca_{0.2}TiO_3.0.5CaCu_3Ti_4O_{12}$, was prepared by the mixing of individual materials of $Ba_{0.8}Ca_{0.2}TiO_3$ and $CaCu_3Ti_4O_{12,}$ through the chemo-mechanical method. The starting materials included analytical grade chemicals, such as Ba $(NO_3)_3$· (99%, Sigma Aldrich), Cu $(NO_3)_2 \cdot 3H_2O$ (99.0%, Junsei), TiO_2 (99.0%, Sigma Aldrich), and glycine (99.0%, Daejung) were taken in their stoichiometry ratios. Solid TiO_2 was used to avoid the use of water-insoluble TiO_2 and cost-bearing titanium isopropoxide, Ti $(OR)_4$. The above-mentioned starting materials were mixed with deionized double distilled water in a beaker containing Ba^{3+}, Cu^2 ions and the obtained solution was heated between 70 °C and 80 °C by using hot plate magnetic stirrer. After evaporation of the water, the resulting precursor of $Ba_{0.8}Ca_{0.2}TiO_3$powder was calcined at 800°C for 8h in a muffle furnace. A similar synthesis procedure has been taken into account for the preparation of $CaCu_3Ti_4O_{12}$ ceramic. A calculated amount of calcined powder $Ba_{0.8}Ca_{0.2}TiO_3$ and $CaCu_3Ti_4O_{12}$ were collected and mixed by using a pestle and mortar in ethanol solution and ground for 12h, for composite formation. The resulting precursor was used to make pellets by applying 4-5 tons of pressure using polyvinyl alcohol as a binder. Finely, The pellets were sintered at two different temperatures namely 950 ºC and 1000 °C for 15 h after removal of binder on heating rate of 500 °C for 2 h.

Table 1. Comparison of properties of BCT-CCTO with properties of other ceramic materials.

Property	BCT-CCTO	$BaTiO_3$ (BT)	$CaCu_3Ti_4O_{12}$ (CCTO)	$SrTiO_3$ (STO)	Pb (Zr_xTi_1) O_3 (PZT)
Composition	Composite of ferroelectric BCT and high-dielectric CCTO	Ferroelectric perovskite	Giant dielectric perovskite	Perovskite structure, paraelectric	Ferroelectric perovskite
Dielectric Constant	High (10^3–10^4, frequency-dependent)	Moderate (10^3 near Curie temp)	Extremely high (>10^4, low freq.)	Moderate (~300–500)	High (500–5000, depending on Zr/Ti)
Dielectric Loss (Tan δ)	Moderate, decreases with frequency	Low (~0.01–0.05)	Moderate to high (0.1–0.2)	Very low (~0.001–0.005)	Moderate (~0.02–0.05)
Frequency Dependence	Significant at low and intermediate frequencies	Stable at low frequencies	Strong dispersion at low frequencies	Stable across a broad frequency range	Stable but dependent on doping
Temperature Stability	Moderate; influenced by Curie temp. of BCT	Limited by Curie temperature (~120°C)	High stability across temperatures	Excellent stability at low temp.	Limited by Curie temp. (100–350°C)
Curie Temperature (T^c)	~80–100°C (BCT phase dominates)	~120°C	No distinct T^c (paraelectric behavior)	~0 K (quantum paraelectric)	100–350°C, depending on composition
Grain Boundary Effects	Strong; IBLC effect enhances permittivity	Minimal	Dominant contributor to dielectric	Minimal	Minimal
Electrical Conductivity	Moderate (thermally activated)	Low	High at grain boundaries	Low	Moderate (depends on doping)
Sintering Temperature	~1000–1200°C	~1200°C	~1100–1150°C	~1300°C	~1000–1250°C
Applications	Capacitors, sensors, energy storage	Capacitors, piezoelectric devices	High-dielectric capacitors, resistors	Tunable devices, quantum electronics	Actuators, transducers, energy storage

Characterization

The formation of phase was confirmed by an X-ray diffractometer (Rigakuminiflex 600, Japan) with Cu-$K_{\alpha,}$ radiation at a scanning rate of 1-2°/min. The particle size was observed by a transmission electron microscope (FEI TECANI G^2 20 TWIN; USA). The sample of BCT-CCTO powder for TEM analysis was prepared in acetone using ultrasonication and after being applied to the carbon-coated copper grid, the BCT-CCTO composite suspensions were dried over 60 °C for 4 h in a hot air oven. A scanning electron microscope (SEM, ZEISS; model EVO-18 research, Germany) was used to describe the microstructure of the composite. The elemental analysis of the BCT-CCTO composite was carried out by EDX (EDX, Oxford instrument, USA). The dielectric properties of the BCT-CCTO composite were measured by an LCR meter (PSM 1735, NumetriQ 4th Ltd., and UK) in a wide range of temperature (300 - 500 K) and frequency (100 Hz - 5 MHz).

RESULTS AND DISCUSSION

X-Ray Diffraction Pattern

The XRD patterns of $0.5Ba_{0.8}Ca_{0.2}TiO_3.0.5CaCu_3Ti_4O_{12,}$ composites are illustrated in Fig. 1(a & b). It is seen that the sintered compound at 950 °C consists of multiple phases of CTO (JCPDS:86-1393), BCTO (JCPDS:80-1343), and the small peak of CuO with JCPDS card N. 48-1548, as described in Fig. 1(b). On the other hand, single-phase formation occurs in the composite materials at the sintering temperature of 1000° C for 15 h (Figure 1a). All XRD patterns were well-indexed on the basis of body-

centered cubic structure with space group Im3, emphasized composite formation of BCT–CCTO without any occurrence of other impurities. The value of crystallite size (D) from XRD data determined with the help of Debye-Scherrer formula is demonstrated by the Cauchy component of the Voigt function in the single-line analysis approach and its value (D) are also ascertained by using a line-broadening technique to XRD data. The Debye-Scherrer equation is represented by the following expression [23].

$D = k\lambda / \beta \cos \theta$

where λ is the wavelength of the X-ray, k is a constant equal to 0.90, θ is the diffraction angle, and β is the full width at half-maximum (FWHM). β is determined for the three most intense XRD peaks. The average crystallite size obtained from the XRD data is 48.14nm.

Microstructure

The SEM image of the BCT–CCTO nanocomposite shown in Figure 2a and b, reveals bimodal type morphology in which grain si are in the order of several hundreds of nanometers. Furthermore, the morphology showed well-packed grains with their high densification without any porosity in the material. The BCT–CCTO ceramic's average grain size was determined using Image J software to be within a range of 98±5 nm. Similar morphology is also observed in the specific portion of SEM image as depicts in Fig. 3(a). The average grain size estimated to be 1.80 ±0.5 µm on the scale of 10 µm. The EDX mapping exhibits the homogeneous distribution of the elements in the specific portion of the BCT-CCTO composite selected for the mapping studies as indicated by Fig. 3(b-f), is also confirmed the existence of Ba, Ca, Ti, Cu, and O elements that indicates the good quality of the chemo-mechanical synthesis.

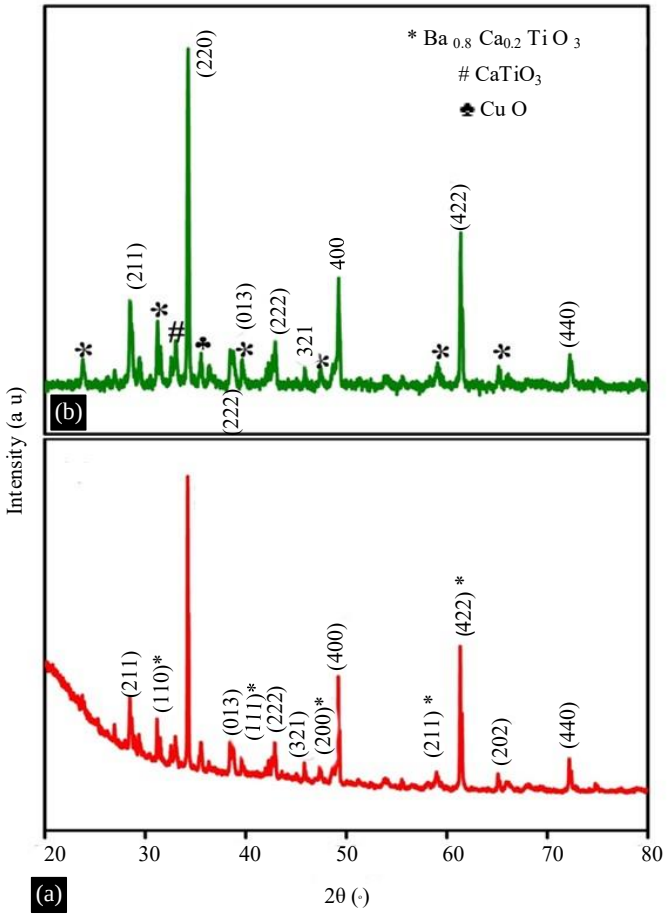

Figure 1. X-ray powder diffraction pattern of BCT-CCTO composite sintered at (a) 950 °C for 15h and (b) sintered at 1000°C for 15 h.

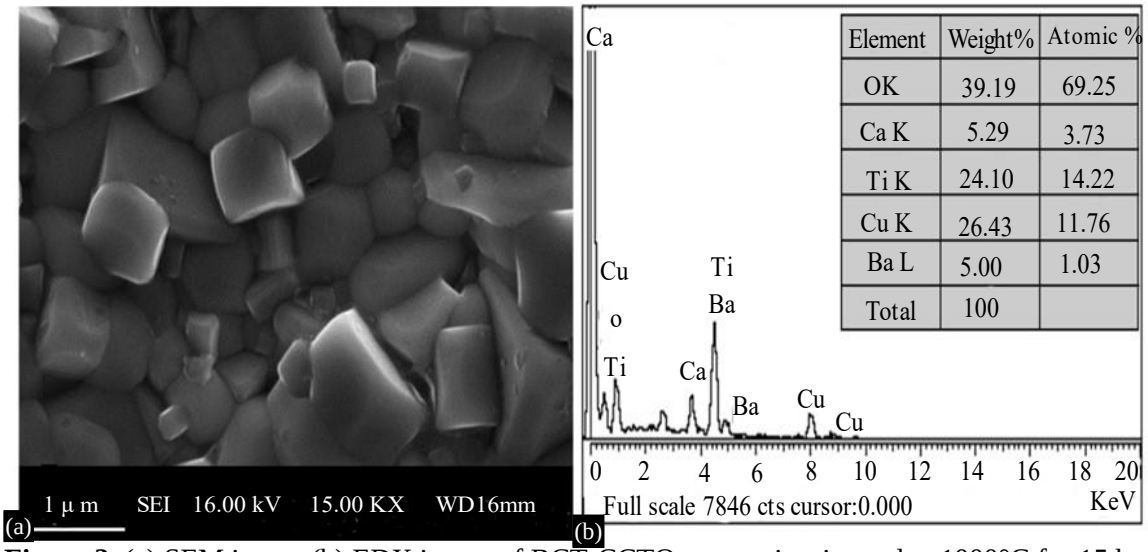

Figure 2. (a) SEM image (b) EDX image of BCT-CCTO composite sintered at 1000°C for 15 h.

The oxidation state and the elemental composition of the sintered composite (BCT-CCTO) at the sintering temperature of 1000 °C for 15 h was investigated through XPS spectrum using Gaussian–Lorentzian profile fitting. This spectrum was recorded by considering the carbon C 1s as a reference peak with the binding energy (B.E) at 285 eV. The presence of all the peaks of the elements Ca 2p, Cu 2p, Ti 2p and O 1s is observed at specific positions in the XPS spectrum as inferred from Figure 4(a) and Figure 4(b) shows the peak of C 1s peak, which confirms the above EDX result and purity of this ceramic synthesized by this route. Figure 4(c & d) represents core level XPS spectra of Ca 2p and Ti 2P. It is clearly observed from the Figure 4 (c) that two peaks are observed in Ca 2p core level with respective binding energy (B.E) at 345.8 eV and 349.43 eV, which may be due to spin- orbit coupling of Ca $2p_{3/2}$ and Ca $2p_{1/2}$, respectively and another XPS spectrum corresponding to Ti 2p core level as depicts in the Figure 4(d) represents the occurrence of another peaks with respective B.E at 457.68 eV and 463.38 eV of Ti $2p_{3/2}$ and Ti $2p_{1/2}$, respectively. The metal-oxygen bonding (M-O bond) peaks corresponding to O1s is also seen in the XPS spectrum at the B.E of 529.13 eV, is described by Fig. 4(e). Furthermore, the presence of another peak located at B.E. 779.29 eV and 794.63 eV, respectively indicates the peak of Ba 3d and peaks located at 933.36 eV and 961.21 eV, respectively in the Cu 2p spectrum of BCT-CCTO composite may be due to Cu $2p_{3/2}$ and Cu $2p_{1/2}$, respectively. As above observations disclosed in the XPS spectra of BCT-CCTO composite emphasized the existence of +2 oxidation state of calcium and copper whereas an occurrence of +4 oxidation state in the titanium element whose binding energy (B.E) values are similar to earlier reported results of CCTO ceramic [24-25]. The Transmission electron microscopy (TEM) examination was utilized to further establish the its internal structure and offer exact measurements of particle size and shape. The morphology of TEM analysis demonstrates the presence of spherical and homogenous-sized particles that resemble platelets of BCT-CCTO composite materials as illustrated in Figure 5. The particle size of the materials is calculated through Image J software and comes to be 97.14 nm which gives similar results of average grain size obtained from SEM image.

Figure 6(a) showed that the dielectric constant at low frequency increased with an increase in temperature while the increment of dielectric constant was relatively low from 30-299 °C, particularly at higher frequencies. In the frequency, the dielectric constant was almost independent of temperature, which showed that there is a mechanical limitation due to a lack of interfacial polarization at higher frequencies. The large variations of ε' from 30-299 °C at low frequencies were attributed to the increased interfacial polarization and the chemical micro heterogeneities in the sample. Figure 6(b) shows the ε" vs. f at a selected range of temperatures. The broad peak maxima represent typical relaxation behavior. The peak frequency of the relaxation peak decreases with decreasing temperature, which indicates that

thermally activated Debye-like dielectric relaxation, is present in this material [26]. These types of dielectric relaxation behaviors are observed whenever two phases with different electrical conductivities; these give rise to a frequency and temperature dependence of the dielectric relaxation behavior [27-29].

The tan δ values at room temperature from Figure 6(c). The relaxation peaks by thermal activation were also observed in tan δ vs. T plots at low frequencies. The tan δ is strongly temperature dependent, which is a general characteristic of ferroelectric materials [30]. The trends in dielectric constant (ε') and dielectric loss (tan δ) with frequency at some measured temperatures for BCT-CCTO composite as represented by the Figure 7a and b. The dielectric constant value of BCT-CCTO at room temperate is comparable with pure BCT, and CCTO possesses relatively low dielectric loss. The presence of high values of ε'and tan δ in the low-frequency region is due to the influence of interfacial polarization which is generally found in $ACu_3Ti_4O_{12}$ family materials [31].

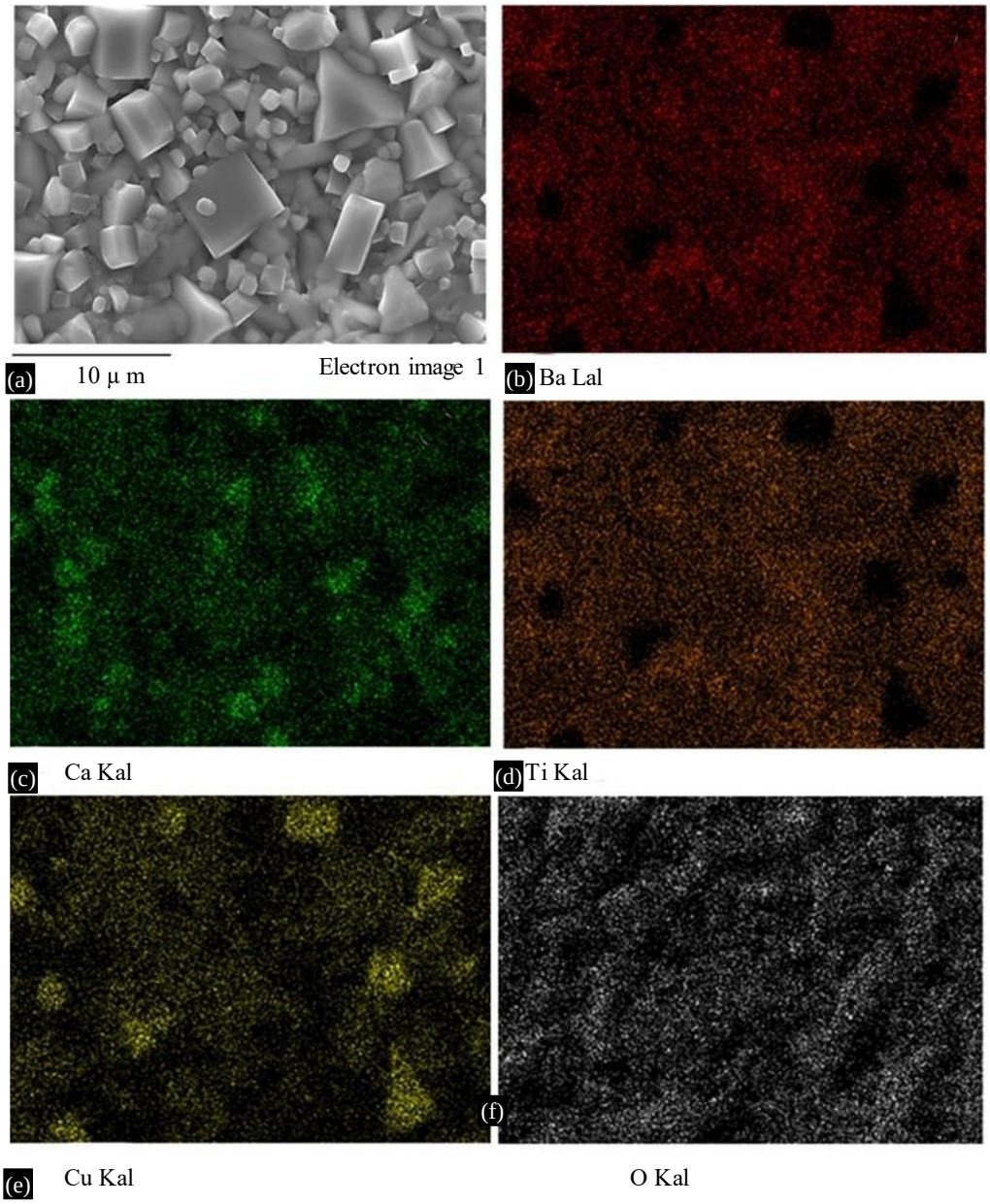

Figure 3. Specific portion of SEM image and EDX mapping of BCT-CCTO composite materials.

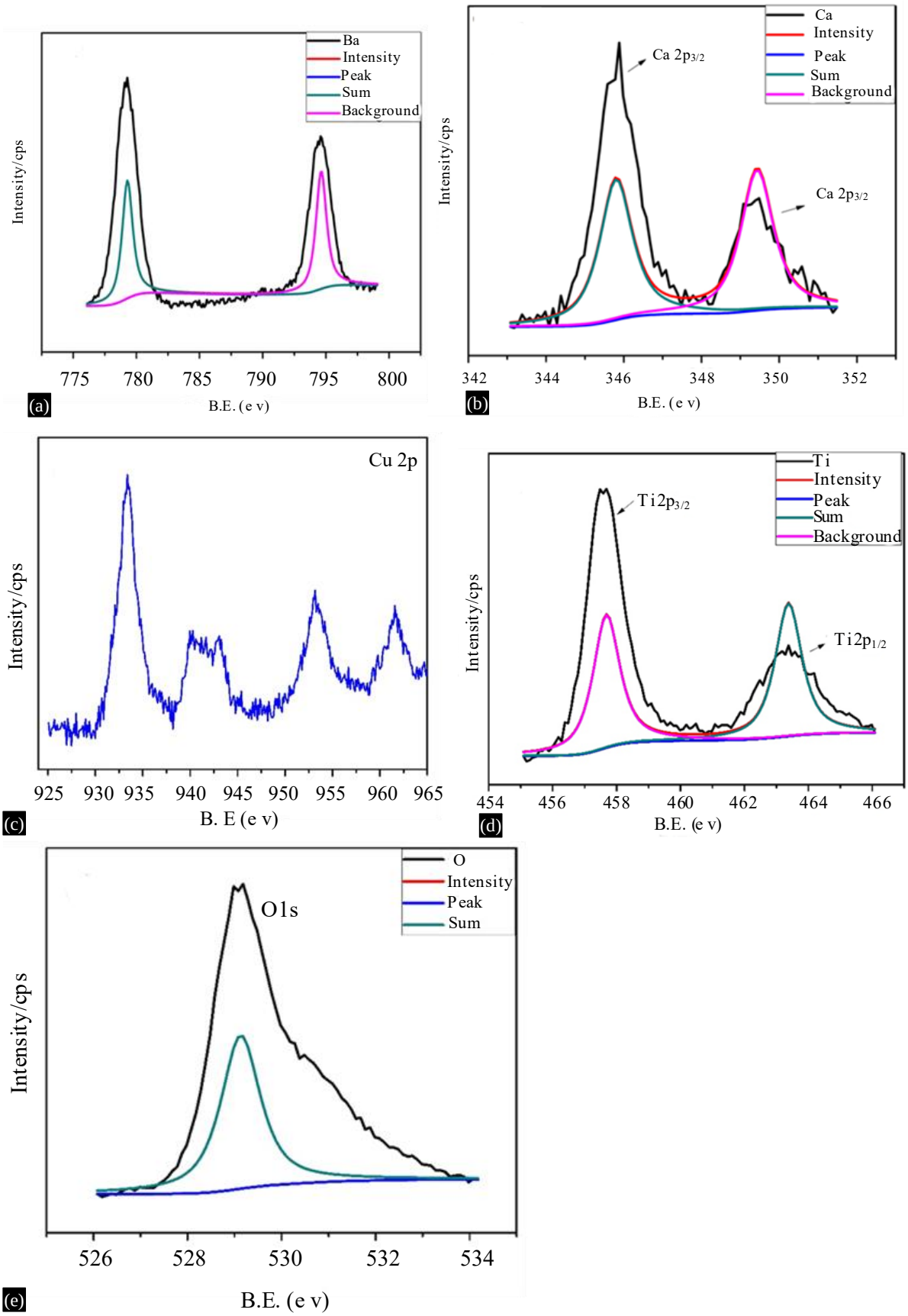

Figure 4. XPS characterization of BCT-CCTO composite sintered at 1000°C for 15 h.

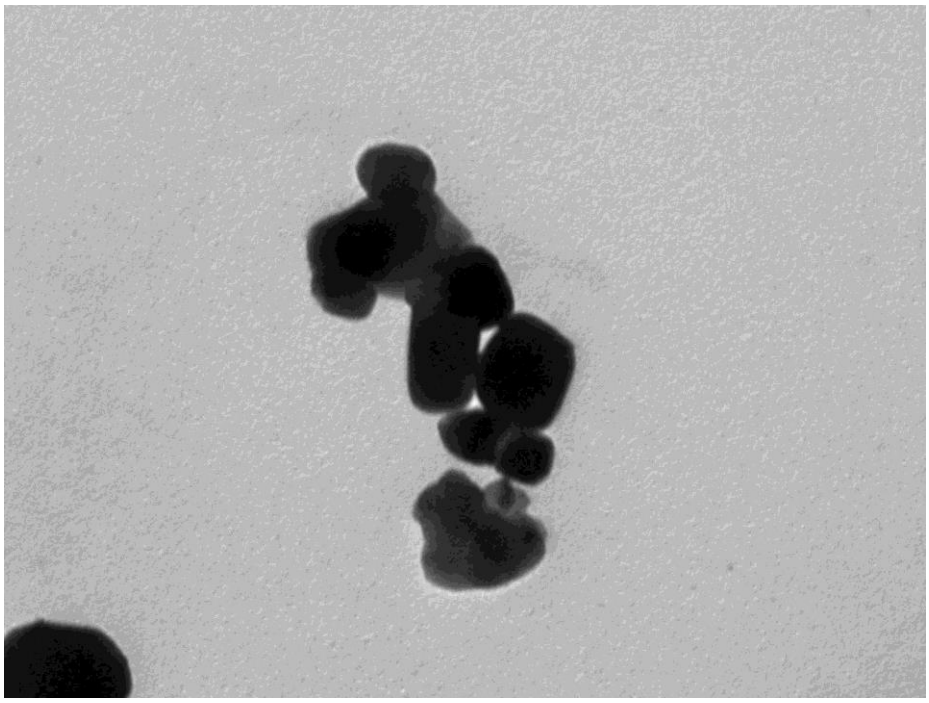

Figure 5. TEM image of BCTCCTO composite sintered at 1000°C for 15 h.

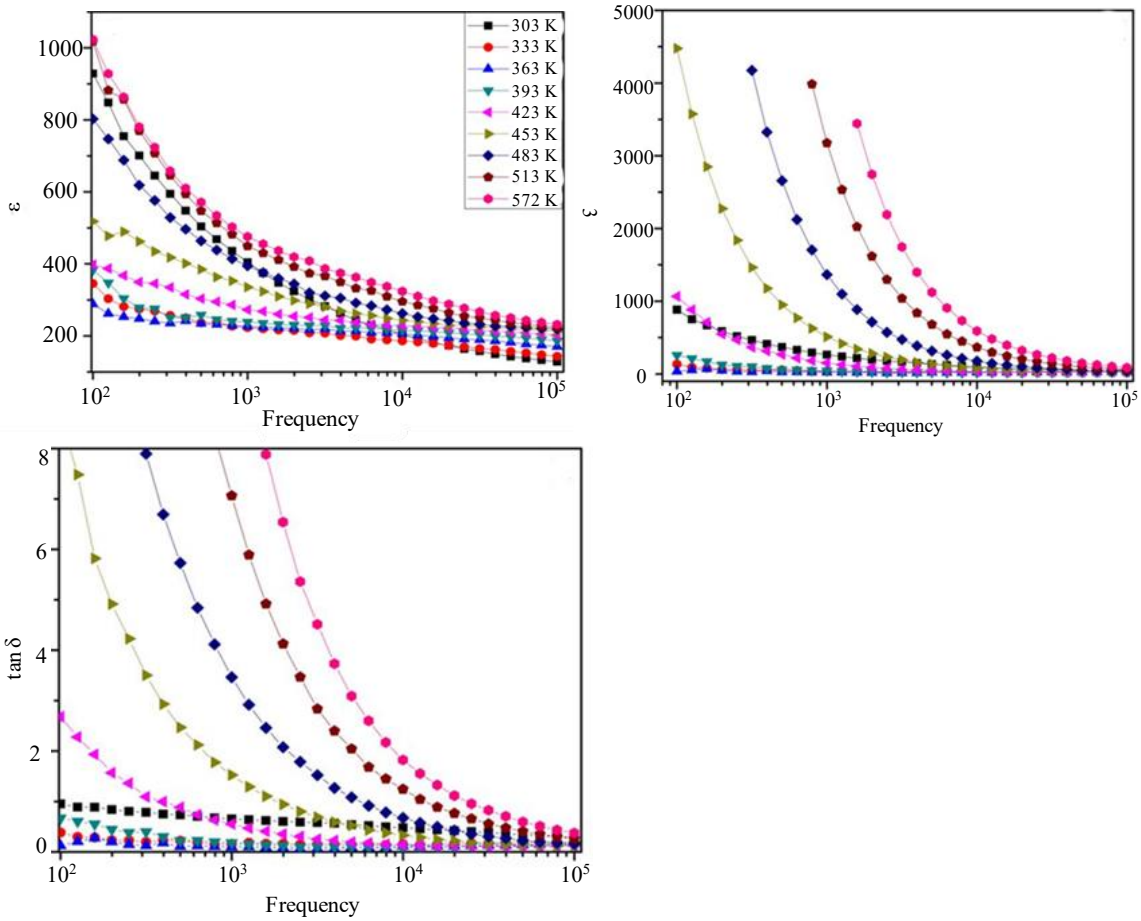

Figure 6. Plots of (a) the dielectric constant (ε'), (b) the Imaginary dielectric constant, and (c) dielectric loss (tanδ) as a function of the temperature of BCT-CCTO composite sintered at 1000 °C for 15 h at different frequencies.

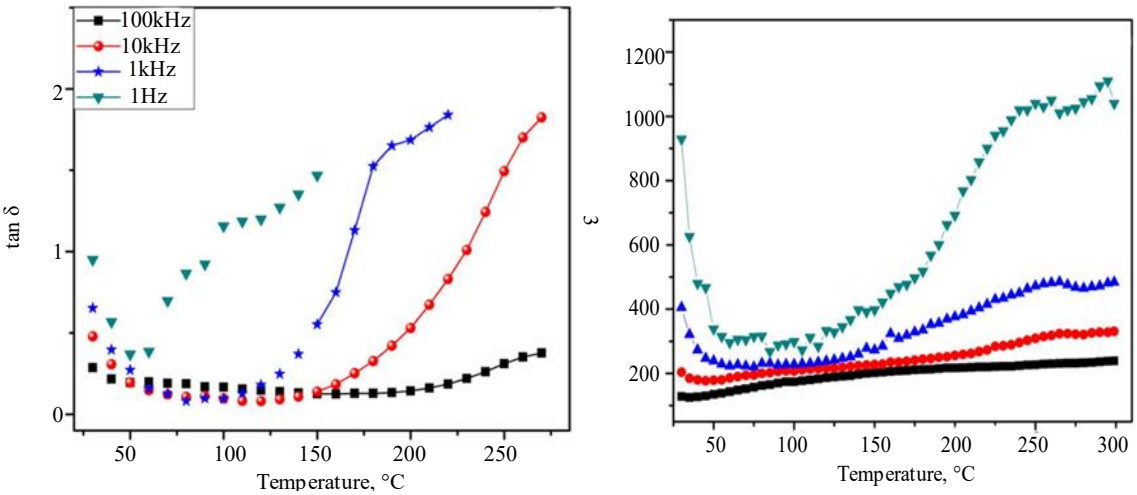

Figure 7. Plots of (a) dielectric loss (tanδ)(b) the dielectric constant (ε') with a temperature of BCTCCTO composite sintered at 1000 °C for 15 h at different frequencies.

CONCLUSIONS

The dielectric constant of BCT-CCTO composites was investigated in this work. In this study, pure-$Ba_{0.8}Ca_{0.2}TiO_3$ and $CaCu_3Ti_4O_{12}$ ceramics with high-performance dielectric properties were prepared via a chemo-mechanical route using a titanium source. XRD analysis confirmed the phase formation of composite material at 1000°C for 15h. The micro-structural properties and elemental composition were confirmed by SEM TEM and EDX morphology. The study dielectric constant, the imaginary dielectric constant, and the tan delta were studied at different frequencies and temperatures. The value of the high dielectric constant is 1025 at high temperature with low frequency and the imaginary dielectric constant show 4494 at low frequency and high temperature. The tan delta value is very low at 100KHz (0.36). The dielectric constant was increased with temperature due to interfacial polarization. The peak frequency of the relaxation peak decreases with decreasing temperature, which indicates that thermally activated Debye-like dielectric relaxation is present in the material.

Acknowledgements

All the authors are grateful to the concerned Institute and University and those for extending support to prepare this Research article.

Declaration of Conflict of Interest

The authors declare that there is no conflict of interest.

REFERENCES

1. K.R. Reddy, H.M. Jeong, Y. Lee, A.V. Raghu, J. Polym. Sci. A: Polym.Chem. 48, 1477–1484. (2010).
2. K.R. Reddy, B.C. Sin, K.S. Ryu, J. Noh, Y. Lee, Synth. Met. 159,1934–1939 (2009).
3. K.R. Reddy, B.C. Sin, C.H. Yoo, W. Park, K.S. Ryu, J.S. Lee, D. Sohn, Y. Lee, Sr. Mater. 58, 1010–1013(2008).
4. K.R. Reddy, B.C. Sin, C.H. Yoo, D. Sohn, Y. Lee, J. Colloid Interface Sci.340, 160–165(2009).
5. K.R. Reddy, B.C. Sin, K.S. Ryu, J.C. Kim, H. Chung, Y. Lee, Synth. Met.159, 595–603(2009).
6. K.R. Reddy, K.P. Lee, J.Y. Kim, Y. Lee, J. Nanosci. Nanotechnol. 8,5632–5639(2008)
7. K.R. Reddy, K.P. Lee, J.Y. Kim, Y. Lee, A.I. Gopalan, Mater. Lett. 62, 1815–1818(2008).
8. L. Singh, U.S. Rai, K.D. Mandal, B.C. Sin, H. Lee, H. Chung, Y. Lee,Mater. Charact. 96,54–62(2014).
9. L. Singh, I. Kim, B. Cheol Sin, A. Ullah, S. K. Woo, Y. Lee, Mater. Sci. Semi. Process. 31, 386–396(2015)

10. S. Krohns, P. Lunkenheimer, S.G. Ebbinghaus, A.Loidl, Appl. Phys. Lett. 91, 022910–022913 (2007).
11. L. Singh, M. Sheeraz, M. N. Chowdhury, U. S. Rai, S. S. Yadava, Y. S. Park, S. V. Singh, Y. Lee, J.Materi. Sci.Materi. in Electro, 29, 10082–10091 (2018).
12. C.C. Home, T. Vogt, S.M. Shapiro, S. Wakimoto, A.P. Ramirez, Science, 293, 673–676 (2001).
13. M. Li, X.L. Chen, D.F. Zhang, W.Y. Wang, W.J. Wang, Sens. Actuators B147,447–452(2010).
14. S. Kwon, C.C. Huang, E.A. Patterson, D.P. Cann, E.F. Alberta, Mater. Lett. 62,633–636 (2008).
15. L. Singh, U.S. Rai, K.D. Mandal, Nanomater. Nanotechnol. 1, 59–66 (2011).
16. S.Y. Cheng, I.D. Kim, S.J. Kang, Nat. Mater. 3, 774–778(2004).[15] G. Du, W. Li, Y. Fu, N. Chen, C. Yin, M. Yan, Mater. Res. Bull. 43,2504–2508 (2008).
17. A.R. Darvishia, W.L. Li, O.S. Bishe, L.D. Wang, Y. Zhao, S.Q. Zhang, W.D. Fei, J. Alloy. Compd. 514,179–182 (2012).
18. L. Singh, U.S. Rai, K.D. Mandal, B.C. Sin, S.I. Lee, Y. Lee, Ceram. Int. 40,10073–10083 (2014).
19. J. Jumpatam, B. Putasaeng, T. Yamwong, P. Thongbai, S. Maensiri,J. Am. Ceram. Soc. 1,1–4(2014).
20. J. Yuan, Y.H. Lin, H. Lu, B. Cheng, C.W. Nan, J. Am. Ceram. Soc. 94,1966–1969(2011).
21. K. Roleder, I. Franke, A.M. Glazer, P.A. Thomas, S. Miga, J. Suchanicz,J. Phys: Condens. Matter 14, 5399–5406(2002).
22. B.Górnicka, B. Mazurek, W.Mielcarek,K.Prociów, J.Warycha,Solid State Pheno. 128, 13-20 (2007).
23. P. Gautam, A. Khare, S. Sharma, N. B. Singh, K. D. Mandal, Prog. in Nat. Sci. Mater. Inter. 26, 567–571 (2016).
24. S. Sarkar, B.K. Chaudhuri, H.D. Yang, J. Appl. Phys. 108, 014114-014115(2010).
25. C.M. Guinness, J.E. Downes, P. Sheridan, P.A. Glans, K.E. Smith, W. Si, P.D. Johnson, Phys. Rev. B 71,195111-195119(2005).
26. P. Liang, Y. Li, X. Chao, Z. Yang, Mater. Res. Bull. 60,212-216(2014).
27. J.Y. Li, X.T. Zhao, S.T. Li, M.A. Alim, J. Appl. Phys 108,104104-104106(2010).
28. W. Li, R.W. Schwartz, Appl. Phys. Lett. 89,242906-242913(2006).
29. K. Meeporn, T. Yamwong, S. Pinitsoontorn, V. Amornkitbamrung, P. Thongbai,Ceram. Int. 40,15897-15906(2014).
30. L. Singh, U.S. Rai, K.D. Mandal, J. Alloy. Compd. 555, 176–183(2013).
31. D.C. Sinclair, and A.R. West, J. of Apple.Phys. 66, 3850 (1989).

